Figure S1 (related to Figures 2 and 3)

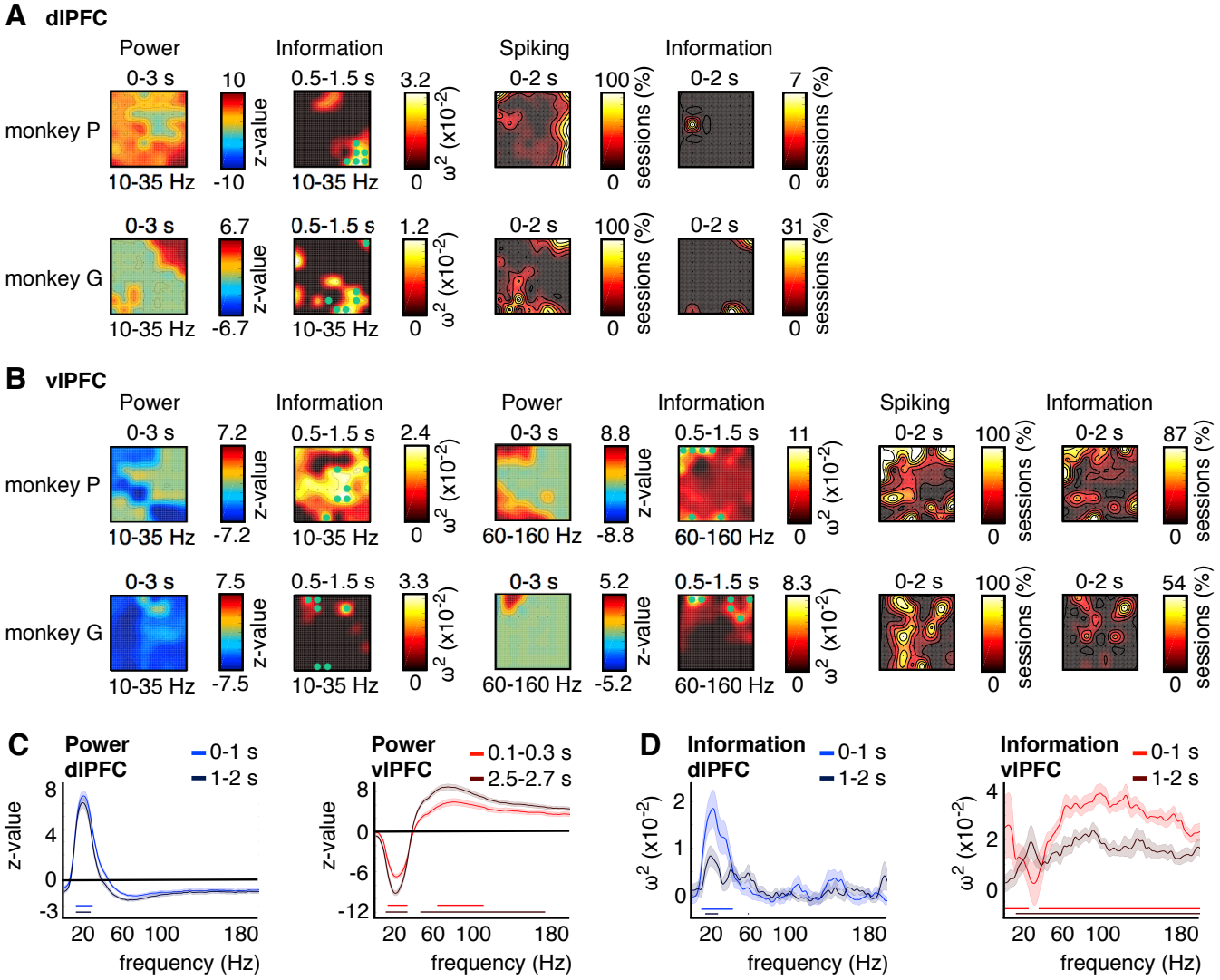

Figure S1. LFP-power, spiking and category information

(**A**) dlPFC-array topographies for beta power changes (z-value), for category information (ω^2) in beta power, for spiking (% recording days with spike rate / s > 1) and category information in spiking (% recording days with $p < .001$). For monkey P (upper row), 80% channels showed a power increase, 25% channels showed category information in power, 20% channels recorded spikes and 0.2% channels / 0.5% MUA channels contained category information in spiking. For monkey G (lower row), 23% channels showed a power increase, 25% channels showed category information in power, 17% channels recorded spikes and 1% channels / 8% MUA channels contained category information in spiking. (**B**) vlPFC-array topographies for beta power changes (z- value), for category information (ω^2) in beta power, for gamma power changes (z- value), for category information (ω^2) in gamma power, for spiking (% recording days) and category information in spiking (% recording days). For monkey P (upper row), 42% channels showed a beta power decrease, 86% channels showed category information in beta power, 34% channels showed a gamma power increase, 95% channels showed category information in gamma power, 40% channels recorded spikes and 24% channels / 51% MUA channels contained category information in spiking. For monkey G (lower row), 95% channels showed a beta power decrease, 13% channels showed category information in beta power, 5% channels showed a gamma power increase, 47% channels showed category information in gamma power, 27% channels recorded spikes and 7.5% channels / 20% MUA channels contained category information in spiking. For (**A, B**), non-significant effects are masked (z-scores with $p < .05$, Bonferroni corrected; ω^2 with $p < .001$; spike rate with spikes / s > 1). The green dots show the 6 channels (10%) with most category information in each frequency band and area, which were used as regions of interest for the distortion / spike-LFP coherence analyses. (**C**) Power change (z-value) relative to baseline as a function of frequency averaged over time intervals of interest (light, dark hue) and all channels in dlPFC (blue) and vlPFC (red). Shaded areas show +/-1 SE. Horizontal lines show significant frequency ranges ($p < .05$,

Bonferroni corrected). (**D**) Category information (ω^2) in power as a function of frequency averaged over significant channels in dlPFC (blue) and vlPFC (red) separately for sample (0-1 s; light hue) and delay epochs (1-2 s; dark hue). Shaded areas show +/-1 SE. Horizontal lines show significant frequency ranges ($p < .001$).

Figure S2 (related to Figure 3)

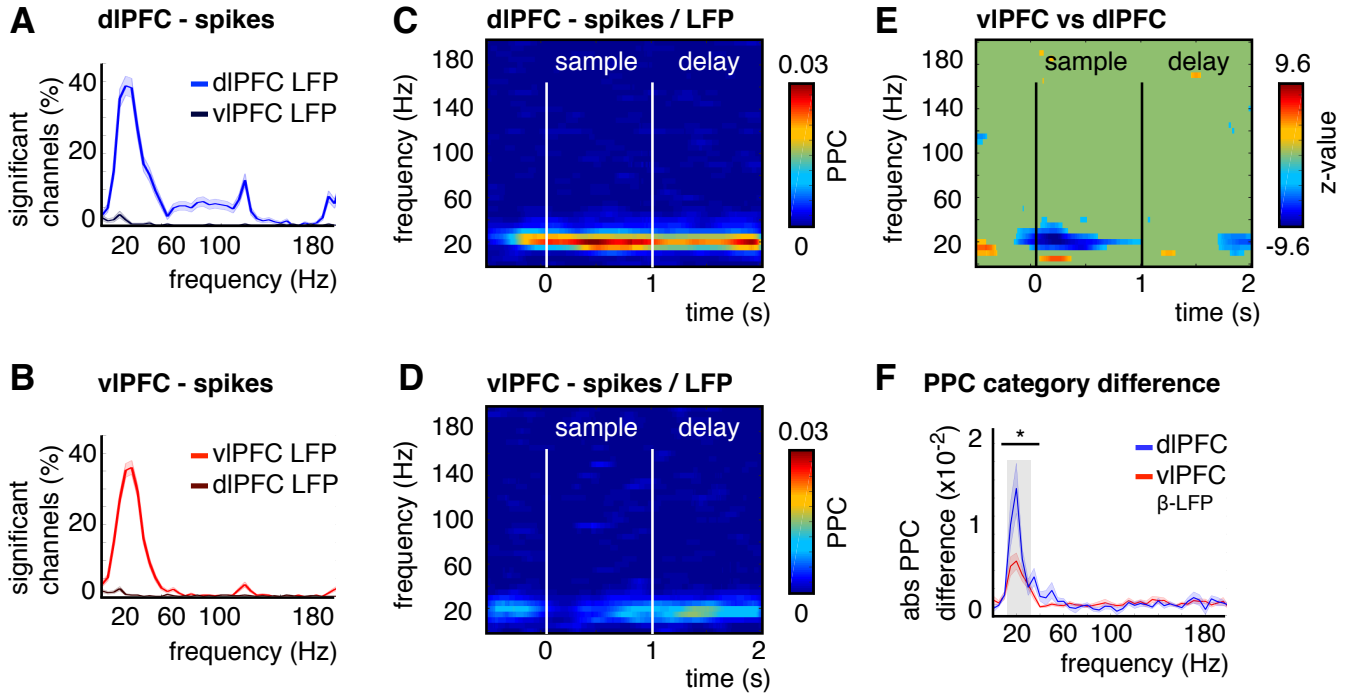

Figure S2. Spike-LFP coherence

(**A, B**) Spike-LFP phase coherence (% significant MUA channels, Rayleigh test $p< .05$, Bonferroni corrected) for spikes between 0-2 s after sample onset (averaged over all LFP channels except for the MUA channel) for dlPFC-spikes to dlPFC-LFP (light blue); dlPFC-spikes to vlPFC-LFP (dark blue, (**A**)) and vlPFC-spikes to vlPFC-LFP (light red); vlPFC-spikes to dlPFC-LFP (dark red (**B**)). Shaded areas show +/-1 *SE.* 64% dlPFC MUA channels showed significant spike-LFP coherence (over all frequencies between 1-200 Hz) for dlPFC-LFP, 10% dlPFC MUA channels for vlPFC-LFP, 60% vlPFC MUA channels for vlPFC-LFP, 10% vlPFC MUA channels for dlPFC-LFP. 32.5% dlPFC MUA channels showed significant spike-LFP coherence averaged over the beta band (10-35 Hz, $p< .001$) for dlPFC-LFP, 0.3% dlPFC MUA channels for vlPFC-LFP, 27.5% vlPFC MUA channels for vlPFC-LFP, 0 vlPFC MUA channels for dlPFC-LFP. (**C, D**) Spike-LFP within-area coherence (pair-wise phase consistency (PPC)) as a function of time and frequency for dlPFC-spikes to dlPFC-LFP (**C**) and vlPFC-spikes to vlPFC-LFP (**D**) for all MUA channels with significant beta band coherence in each area. (**E**) Difference in spike-LFP within-area coherence (PPC) between vlPFC and dlPFC (Mann-Whitney U-test, z-value) as a function of time and frequency for all MUA channels with significant beta band coherence in each area. Non-significant z-values ($p< .001$) are masked. (**F**) Absolute PPC difference between categories (for 0-2 s) over frequency averaged over all significant MUA channels in the beta band (gray area). The median absolute PPC difference from the category-shuffled permutation distributions was subtracted from the observed absolute PPC difference per MUA channel. Shaded areas show +/-1 *SE.* Asterisks indicate the significance level (with * $p< .05$). The PPC differences were calculated for the 10% most category-informative LFP electrodes for dlPFC / vlPFC-beta power (see Figure S1). For comparison, Figure 3F shows the data for the 10% most category-informative LFP electrodes for vlPFC-gamma power. For the vlPFC-beta LFP, 9.2% vlPFC MUA channels showed significant PPC differences between categories ($p< .05$ permutation test, frequency-cluster corrected for 1-200 Hz). For beta PPC differences, there were 8.9% significant vlPFC MUA channels (vs. 5%, $p< 4.3x10^{-5}$).

Figure S3 (related to Figure 4)

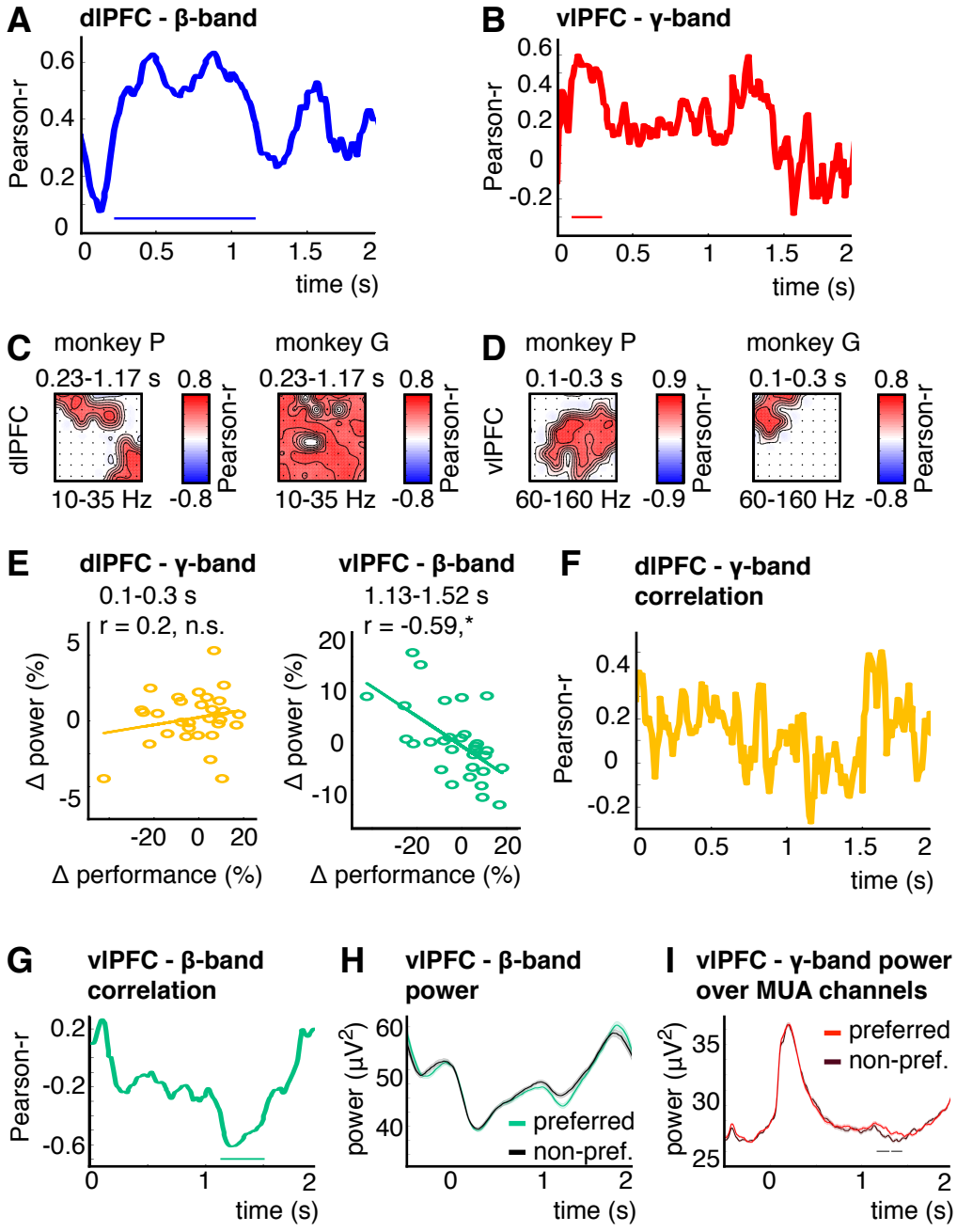

Figure S3. Correlation between performance differences and power differences

(**A, B)** Pearson-correlation coefficient (r) over time between behavioral performance differences and power differences between categories averaged in the beta band (10-35 Hz) and all electrodes in dlPFC ((**A**), blue) and the gamma band (60-160 Hz) in vlPFC ((**B**), red). Horizontal lines show significant time intervals (time-cluster corrected; for dlPFC beta $p < .002$ for 0.23-1.17 s; for vlPFC gamma $p < .02$ for 0.1-0.3 s). (**C, D**) Array topographies for the correlation (Pearson-r) between performance differences and power differences between categories averaged over the beta band (10-35 Hz) in dlPFC (**C**) or the gamma band (60-160 Hz) in vlPFC (**D**) and over the time interval of interest (see (**A, B**)). Non-significant Pearson-r coefficients are masked (dlPFC beta: 30% electrodes (two clusters) with $p < .018$ and $p < .028$ for monkey P; 92% electrodes with $p < .002$ for monkey G; vlPFC gamma: 42% electrodes with $p < .006$ for monkey P, 14% electrodes with $p < .006$ for monkey G, channel-cluster corrected). (**E**) dlPFC-gamma power difference (yellow) and vlPFC-beta power difference (green) between categories plotted against performance difference between categories per session. Straight lines show the linear fit. Asterisks indicate the significance level (with n.s. = not significant, * p< .05). dlPFC-gamma power differences were averaged between 0.1-0.3 s, where we found a significant effect for vlPFC-gamma power (see (**B**)). vlPFC-beta power differences were averaged over the significant time interval shown in (**G**). (**F, G**) Pearson-correlation coefficient (r) over time between behavioral performance difference and dlPFC-

gamma (yellow, (**F**)) and vlPFC-beta (green, (**G**)) power differences between categories (averaged over all electrodes per area). Horizontal lines show significant time intervals (time-cluster corrected; for vlPFC beta $p < .016$ for 1.13-1.52 s). For dlPFC-gamma power (**F**), there was no significant correlation over time. (**H**)) vlPFC**-**beta power for preferred / non-preferred categories (averaged over channels with a significant correlation). Shaded areas show +/-1 *SE*. (**I**) vlPFC-gamma power for preferred / non-preferred categories averaged over all channels that contained significant category information for spiking (242 MUA channels). Horizontal lines show significant time intervals ($p < .028$ for 1.16-1.44 s, time-cluster corrected). For comparison: Figure 4F shows vlPFC-gamma power averaged for each recording day over electrodes with a significant correlation between power-performance differences (see (**D**)). Figure 4G shows the spike rate averaged over all electrodes that contained significant category information for spiking (like in (**I**)). Shaded areas show +/-1 *SE* with $N = 242$ MUA channels in (**I**) and Figure 4G. $N = 30$ recording days in Figure 4F.

Figure S4 (related to Figures 5 and 6)

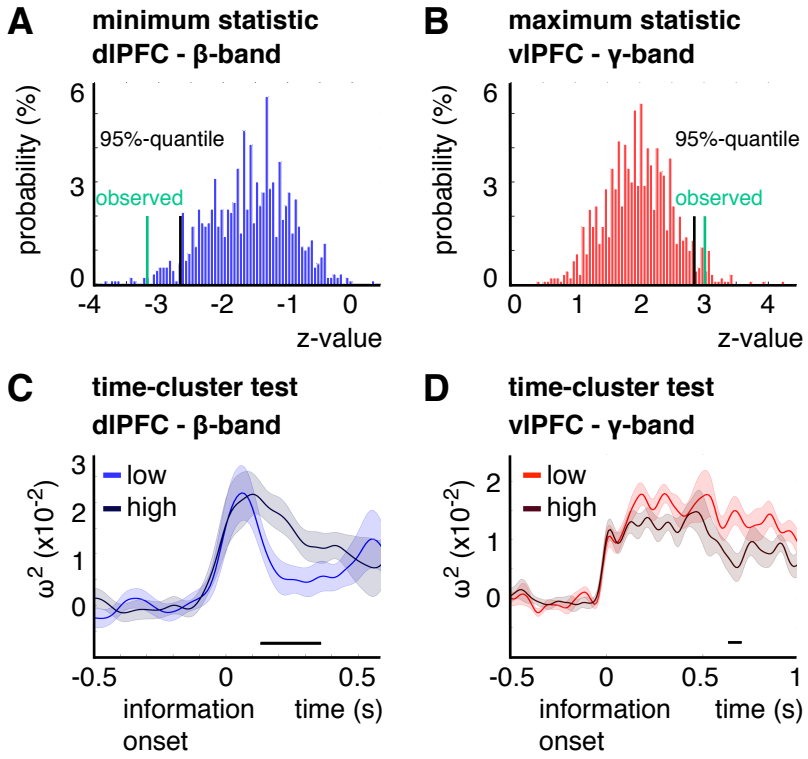

Figure S4. Category information for different distortion levels per task epoch

(A) Permutation distribution (Monte-Carlo approximation with 1000 runs) for the minimum / maximum statistic (Wilcoxon z-value) for the difference between low and high distortion with shuffled condition labels for category information in dlPFC-beta power during the delay ((A), blue) and vlPFC-gamma power during the sample epoch ((B), red). The black vertical line shows the 95%-quantile and the green vertical line shows the observed minimum / maximum statistic (dlPFC-beta at $p < .01$; vlPFC-gamma at $p < .027$). (C, D) Category information (ω^2) as a function of time for dlPFC-beta power ((C), blue) and vlPFC-gamma power ((D), red) for low (light hue) and high distortion (dark hue). The time courses were aligned to the first time point with significant category information per recording day ($p < .05$ permutation test). In case there was no time point with $p < .05$ (which happened in dlPFC-beta for 2 / 30 recording days), we aligned to the time point with maximal information. The alignment accounts for variability in the latency of category information due to different categories and exemplars on different recording days. For dlPFC-beta power, the first significant time point varied with a 0.375 s standard deviation (with *mean* = 0.532 s). For vlPFC-gamma power, it varied with a 0.162 s standard deviation (with *mean* = 0.186 s). We tested across all time points that were consistently available across all recording days from the first significant time point per day up to the test exemplar onset (sample and delay epoch). Horizontal lines show significant time intervals (dlPFC-beta $p < .01$ for 0.13-0.36 s; vlPFC-gamma $p < .038$ for 0.63-0.7 s, time-cluster corrected).